Oligomeric State of Wild-Type and Cysteine-Less Yeast Mitochondrial Citrate Transport Proteins[1]

Rusudan Kotaria,[2] June A. Mayor,[2] D. Eric Walters,[2] and Ronald S. Kaplan[2,3]

Experiments have been conducted to determine the oligomeric state of the mitochondrial citrate transport protein (CTP) from the yeast *Saccharomyces cerevisiae*. Both wild-type and cysteine-less (Cys-less) CTPs were overexpressed in *E. coli* and solubilized with sarkosyl. The purity of the solubilized material is approximately 75%. Upon incorporation into phospholipid vesicles, a high specific transport activity is obtained with both the wild-type and Cys-less CTPs, thereby demonstrating the structural and functional integrity of the preparations. Two independent approaches were utilized to determine native molecular weight. First, CTP molecular weight was determined via nondenaturing size-exclusion chromatography. With this methodology we obtained molecular weight values of 70,961 and 70,118 for the wild-type and Cys-less CTPs, respectively. Second, charge-shift native gel electrophoresis was carried out utilizing a low concentration of the negatively charged detergent sarkosyl, which served to both impart a charge shift to the CTP and the protein standards, as well as to promote protein solubility. Via the second method, we obtained molecular weight values of 69,122 and 74,911 for the wild-type and Cys-less CTPs, respectively. Both methods clearly indicate that following solubilization, the wild-type and the Cys-less CTPs exist exclusively as dimers. Furthermore, disulfide bonds are not required for either dimer formation or stabilization. The dimeric state of the CTP has important implications for the structural basis underlying the CTP translocation mechanism.

KEY WORDS: Mitochondria; transporter; dimer; overexpression; membrane protein.

INTRODUCTION

The mitochondrial citrate transport protein (i.e., CTP) from higher eukaryotes catalyzes an obligatory exchange of citrate plus a proton across the mitochondrial inner membrane for either another tricarboxylate + H^+, a dicarboxylate, or phosphoenolpyruvate (Palmieri *et al.*, 1972). Following the efflux of citrate from

the mitochondrial matrix, and the subsequent diffusion of this metabolite through the outer membrane via the voltage-dependent anion channel, the resulting cytoplasmic citrate can then function as a carbon source for fatty acid and sterol biosyntheses, and can also generate NAD^+ for use in glycolysis (Watson and Lowenstein, 1970; Brunengraber and Lowenstein, 1973; Endemann *et al.*, 1982; Conover, 1987). Thus, in higher eukaryotes, the CTP plays an essential role in intermediary metabolism. Because of its importance, the CTP has been extensively characterized. Accordingly, it has been purified in reconstitutively active form (Kaplan *et al.*, 1990; Bisaccia *et al.*, 1989), kinetically characterized (Bisaccia *et al.*, 1990), cloned (Kaplan *et al.*, 1993), and overexpressed (Xu *et al.*, 1995). Recently, the mitochondrial CTP from the yeast *Saccharomyces cerevisiae* has been identified via over-

expression followed by functional reconstitution of the purified protein product (Kaplan *et al.*, 1995).

An important issue, with respect to the CTP translocation mechanism, concerns the oligomeric state of this carrier. Hydropathy analysis of the CTP, as well as other mitochondrial anion carriers, predicts six putative α-helical membrane-spanning domains (for review see Kaplan, 1996). However, most transporters from other membranous sources are somewhat larger than the mitochondrial anion carriers and are thought to contain 10–12 membrane-spanning domains (Maloney, 1990; Marger and Saier, 1993). This has led to the suggestion that the mitochondrial transporters exist as functional dimers. In fact, there is some evidence to support this view. The most well-studied case is the mitochondrial ADP/ATP translocase, where a combination of inhibitor-binding stoichiometry (Riccio *et al.*, 1975), analytical ultracentrifugation (Hackenberg and Klingenberg, 1980), and cross-linking (Majima *et al.*, 1995) studies all point to the solubilized transporter as existing as a homodimer. In an elegant study (Schroers *et al.*, 1998) in which the detergent-solubilized monomers of the phosphate carrier were differentially tagged, it has been shown that the phosphate carrier exists as a stable homodimer. Finally, cross-linking studies carried out with the uncoupling protein (Klingenberg and Appel, 1989) and the α-ketoglutarate carrier (Bisaccia *et al.*, 1996) also suggest a dimeric state.

To date, there has been no published information on the oligomeric state of the mitochondrial CTP. Accordingly we have carried out investigations in which we utilized two independent methods, namely size-exclusion chromatography and charge-shift native polyacrylamide gel electrophoresis to determine the oligomeric state of the yeast mitochondrial CTP. Both methods show that upon overexpression and subsequent solubilization, the wild-type yeast CTP, as well as a site-specifically mutated Cys-less CTP, exist in a dimeric state. Upon incorporation into phospholipid vesicles, both preparations catalyzed BTC-sensitive citrate/citrate exchange with a high specific activity. We conclude that the functional unit of the CTP is a homodimer and that dimer formation and stabilization do not require the presence of disulfide bonds.

EXPERIMENTAL PROCEDURES

Overexpression, Solubilization, and Measurement of Citrate Transport

The wild-type and Cys-less CTPs were overexpressed in *E. coli* exactly as previously detailed (Kaplan *et al.*, 1995; Xu *et al.*, 1995). Following isolation of the inclusion-body fraction, the CTP was solubilized with 1.2% sarkosyl followed by centrifugation at $314,000 \times g$ (max) for 30 min. The resulting supernatant contained the solubilized CTP. Solubilized transporter was incorporated into preformed phospholipid vesicles via the freeze–thaw-sonication technique exactly as previously detailed (Kaplan *et al.*, 1990, 1995). BTC-sensitive [^{14}C]citrate/citrate exchange was measured utilizing 10- to 30-sec transport incubations as previously described (Kaplan *et al.*, 1995).

Size-Exclusion Chromatography

Solubilized CTP preparations (2.0 ml) were applied to a Sephacryl S-300 (26/60) column. The column had been equilibrated in Buffer A [10 mM Tris-HCl, pH 7.6; 150 mM NaCl, 0.3% sarkosyl (Fluka)]. Protein elution was carried out in the same buffer. For all experiments, the flow rate was 1.3 ml/min. Standards were dissolved in Buffer A (2.0 ml) and are listed in Table I as well as the legend to Fig. 1. The K_{av} was calculated according to the formula: $K_{av} = V_e - V_o/V_t-V_o$ where V_e is the elution volume of the sample of interest, V_o is the void volume (i.e., the elution volume of Blue Dextran 2000), and V_t is the total volume of the packed bed (i.e, 320 ml).

Charge-Shift Native Gel Electrophoresis

Protein standards (see Table I and the legend to Fig. 2), as well as preparations of the CTP, were electrophoresed on precast Tris–glycine gels, which were purchased from Novex. Native sample and running buffers were utilized as formulated by Novex (essentially the Laemmli system (Laemmli, 1970) without SDS), except that 0.1% sarkosyl was added to all buffers. Acrylamide concentrations ranging from 8 to 18% (total acrylamide) were utilized and the ratio of total acrylamide to *bis*-acrylamide was approximately 38.5 to 1. Proteins were fixed and stained with Coomassie as previously described (Kaplan *et al.*, 1986). The R_m (i.e., the relative mobility) was calculated as the distance migrated by a given protein/distance migrated by the dye bromophenol blue. Other calculations are described in the text.

Table I. Protein Calibration Standards Used in the Gel Filtration and/or the Native PAGE Studies[a]

Protein	Source	Approximate molecular weight
Myoglobin	Horse skeletal muscle (Sigma M-0630)	17,800
Trypsin inhibitor	Soybean (Sigma T-9003)	22,100
Carbonic anhydrase	Bovine erythrocyte (Sigma C-7025; C-5024)	29,000
Peroxidase	Horse radish (Sigma P-6782)	40,000
Ovalbumin	Chicken egg (Sigma A-8529)	45,000
Albumin (monomer)	Bovine serum (Pharmacia 17-0442A)	67,000
apo-Transferrin	Human (Sigma T-2252)	81,000
Albumin (dimer)	Bovine serum (Pharmacia 17-0442A)	134,000
Alcohol dehydrogenase	Yeast (Sigma A-8656)	150,000
Aldolase	Rabbit Muscle (Pharmacia 17-0441A)	158,000

[a] Molecular weights were obtained from either the manufacturer or from Harlan *et al.*, 1995.

Miscellaneous Procedures

Site-specific mutagenesis of the CTP to generate the Cys-less CTP was carried out utilizing a PCR site-directed mutagenesis system (Gibco BRL) as previously detailed (Xu *et al.*, 1999). The sequence of the final Cys-less CTP was confirmed by double-stranded automated sequencing. The protein content of the solubilized CTP fractions was determined as previously described (Kaplan and Pedersen, 1985).

RESULTS AND DISCUSSION

High Level Expression, Solubilization, and Purification of the Wild-Type and Site-Specifically Generated Cys-less CTPs

To determine the CTP oligomeric state we pursued the following strategy. First, the wild-type and a cysteine-less CTP (which we generated by mutating the four endogenous Cys to either Ser or Val; i.e., C28S/C73V/C192S/C256S) were overexpressed in *E. coli* and solubilized from an isolated inclusion-body fraction with the detergent sarkosyl. The solubilized protein is abundant (i.e., 30–60 mg/L of *E. coli* culture) and is approximately 75% pure at this stage. Furthermore, we have previously shown (Kaplan *et al.*, 1995; Xu *et al.*, 1999) that upon incorporation into liposomal vesicles, both the wild-type and Cys-less CTPs are highly functional (i.e., V_{max} values of 2.7 and 1.7 μmol/min/mg for the wild-type and Cys-less CTPs, respectively). Moreover, they catalyze BTC-sensitive citrate/citrate exchange with essentially native kinetic properties, substrate specificity, and requirement for intraliposomal substrate. Second, we determined the molecular weight of the solubilized CTPs via two independent methods, namely size-exclusion chromatography and charge-shift native gel electrophoresis.
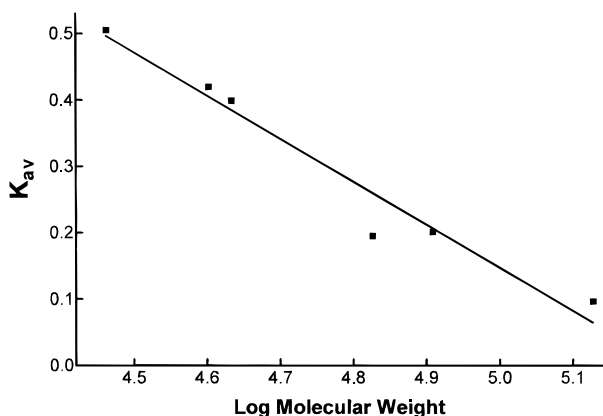

Fig. 1. Molecular mass calibration curve for the size-exclusion Sephacryl S-300 column. The standards used for this calibration curve were: carbonic anhydrase, ovalbumin (Sigma, A-5503; MW = 43,000), peroxidase, bovine serum albumin (monomer and dimer), and apo-transferrin. The equilibration and eluent media consisted of 10 mM Tris-HCl, pH 7.6; 150 mM NaCl, 0.3% (w/v) sarkosyl. The flow rate was 1.3 ml/min. Data represent means of at least duplicate chromatographic runs. A best-fit line was constructed based on linear regression analysis via the methods of least squares. The slope and the Y-axis intercept of the best-fit line were −0.649 and 3.393, respectively. The correlation coefficient was 0.955.
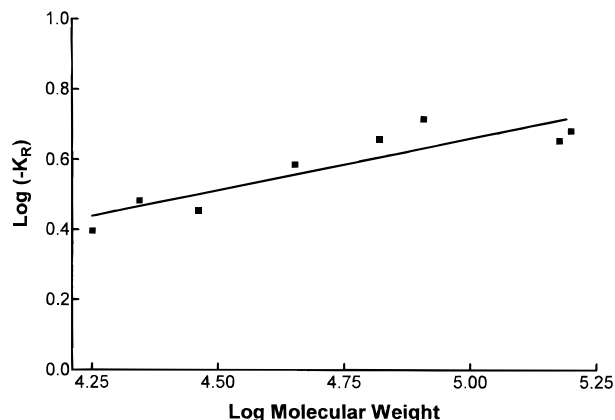
Fig. 2. Linear relationship between the $\log(-K_R)$ and the log molecular weight with protein standards following charge-shift native polyacrylamide gel electrophoresis. The standards used for this calibration curve were: myoglobin, trypsin inhibitor, carbonic anhydrase, chicken egg albumin, bovine serum albumin (Sigma, A-8654; mol. wt. 66,000), apo-transferrin, alcohol dehydrogenase, and aldolase. Each standard was electrophoresed through four to five different polyacrylamide gel concentrations in the range of 8 to 16% (total acrylamide). The relative mobility (i.e., R_m) was determined at each gel concentration and the parameter $100 \log(R_m \times 100)$ was plotted against the acrylamide concentration (i.e., Ferguson plot). A best-fit line was constructed based on linear regression analysis via the methods of least squares. The slope of the line (i.e., K_R) obtained for each standard was then plotted as $\log(-K_R)$ versus log molecular weight in the present figure. The slope and Y-axis intercept of the final best-fit line were 0.294 and -0.813, respectively. The correlation coefficient was 0.806.

Determination of Molecular Weight Via Size-Exclusion Chromatography

Our first approach to determine the molecular weight of the wild-type and Cys-less CTPs involved the use of size-exclusion chromatography (Sephacryl S-300). An advantage afforded by this approach is that it is independent of the native charge of either the standards or the protein of interest and is strictly related to molecular size. Our first goal was to determine whether, using conditions in which the solubilized CTP was stable (i.e., 0.3% sarkosyl), one could obtain a linear relationship between the K_{av} and the log molecular weight for a series of standards in the desired molecular weight range. Figure 1 depicts the standard curve that we obtained employing six protein standards in the molecular weight range of 29,000 to 133,000 Da. A straight line is obtained with a correlation coefficient of 0.955. Having demonstrated this linear relationship, we then determined the elution volume and calculated the K_{av} for the wild-type and the Cys-less CTPs. It

should be noted that in these experiments, after the size-exclusion chromatography the resulting CTP eluate fractions are quite pure (i.e., > 90%). Based on five independent experiments with each CTP form, we obtained molecular weight determinations of 70,961 ± 829 and 70,118 ± 939 (mean ± S.D.) for the wild-type and Cys-less CTPs, respectively. One should note that the actual calculated molecular weight (based on their known amino acid sequences) of the wild-type and Cys-less CTP homodimers are 64,448 and 64,344, respectively. Thus, our results strongly support the postulate that the solubilized CTP exists as a dimer. Moreover, our results with the Cys-less CTP indicate that dimer formation and stabilization do not require the presence of disulfide bonds.

Determination of Molecular Weight Via Charge-Shift Native Gel Electrophoresis

Charge-shift native gel electrophoresis has been utilized as a second, independent approach to determine the native molecular weight of the wild-type and the Cys-less CTP preparations. In this method, a low concentration of the negatively charged detergent sarkosyl (i.e., 0.1%) was added to the running and sample buffers. The sarkosyl served two functions. First, it induced a charge shift on the protein of interest so that all the standards and the CTP migrate in the same direction (i.e., toward the anode). Second, it rendered the CTP soluble and prevented aggregation. Thus protein separation via this methodology is based on a combination of both the net charge and the mass of the protein–sarkosyl complex. Information regarding each of these parameters is obtained by Ferguson analysis (see below). Variations of this general approach have been reported by numerous laboratories (Helenius and Simons, 1977; Newby and Chrambach, 1979; Schagger and von Jagow, 1991). Finally, it is important to note that sarkosyl does not denature the CTP, as judged by the fact that upon reconstitution in phospholipid vesicles the CTP catalyzes BTC-sensitive citrate/ citrate exchange with high specific activity.

We carried out the following experiments. First, a series of standards were electrophoresed at four to five different gel concentrations and their relative mobilities (R_m) were determined. With each standard we then plotted the parameter $100 \log(R_m \times 100)$ versus the polyacrylamide concentration (i.e., a Ferguson plot) (Ferguson, 1964; Hedrick and Smith, 1968; Bryan, 1977) and in every case a straight line was

obtained, with correlation coefficients typically greater than 0.98 (data not shown). The slope of these plots (i.e., the retardation coefficient, K_R) is a measure of the extent of molecular sieving that occurs and is directly related to protein molecular size (Ferguson, 1964; Hedrick and Smith, 1968; Chrambach and Rodbard, 1971; Bryan, 1977). The $\log(-K_R)$ versus the log molecular weight was then plotted and the resulting standard curve is depicted in Fig 2. Utilizing eight standard proteins, which range in molecular weight from 17,800 to 158,000, a straight line was obtained, thereby confirming the linear relationship between $\log(-K_R)$ and log molecular weight under the charge-shift gel electrophoretic conditions. This standard curve was then utilized to determine the molecular weight of the CTP preparations as follows.

With the solubilized wild-type and the Cys-less CTPs, a Ferguson analysis was carried out. Accordingly, electrophoresis was performed at five different gel concentrations and the relative mobility (R_m) of the CTP was measured with each gel concentration. Figure 3 depicts Ferguson plots for both the wild-type and Cys-less CTPs. Linear plots were obtained with a correlation coefficient of 0.993 for both CTP forms. It should be noted that two important parameters are obtained from these plots (Ferguson, 1964; Hedrick and Smith, 1968; Chrambach and Rodbard, 1971; Bryan, 1977). The slope (i.e, the K_R) is directly related to CTP molecular size and enables a determination of CTP molecular weight via interpolation using the

Table II. Summary of Molecular Weight Determinations for the Wild-Type and Cys-less CTPs[a]

	Molecular weight determination		
CTP variant	Size-exclusion chromatography	Native PAGE	Calculated value for dimer
Wild-type	70,961 ± 829	69,122 ± 6494	64,448
Cys-less	70,118 ± 939	74,911 ± 8952	64,344

[a] Molecular weight determination by size-exclusion chromatography was accomplished via use of the calibration curve (Fig. 1) as described in the text. The native PAGE value was obtained by Ferguson plot analysis (Fig. 3) and comparison of the resulting slopes with the calibration curve (Fig. 2) as described in the text. Data are presented as means ± SD, which were obtained from at least five separate determinations. The molecular weight of the wild-type and Cys-less CTP dimers were calculated using the Genetics Computer Group "peptidesort" program.

calibration curve depicted in Fig. 2. We obtained molecular weight values of 69,122 ± 6494 and 74,911 ± 8952 for the wild-type and Cys-less CTPs, respectively (see Table II). The Y-axis intercept (Y_0), a measure of a protein's relative mobility at zero gel concentration, is strictly related to molecular net charge. As expected, extrapolation of the data presented in Fig. 3 to the Y-axis intercept gave essentially identical values for the charge densities of the wild-type and the Cys-less CTPs (i.e., Y_0 values of 230.7 ± 2.5 and 231.3 ± 2.5, respectively).
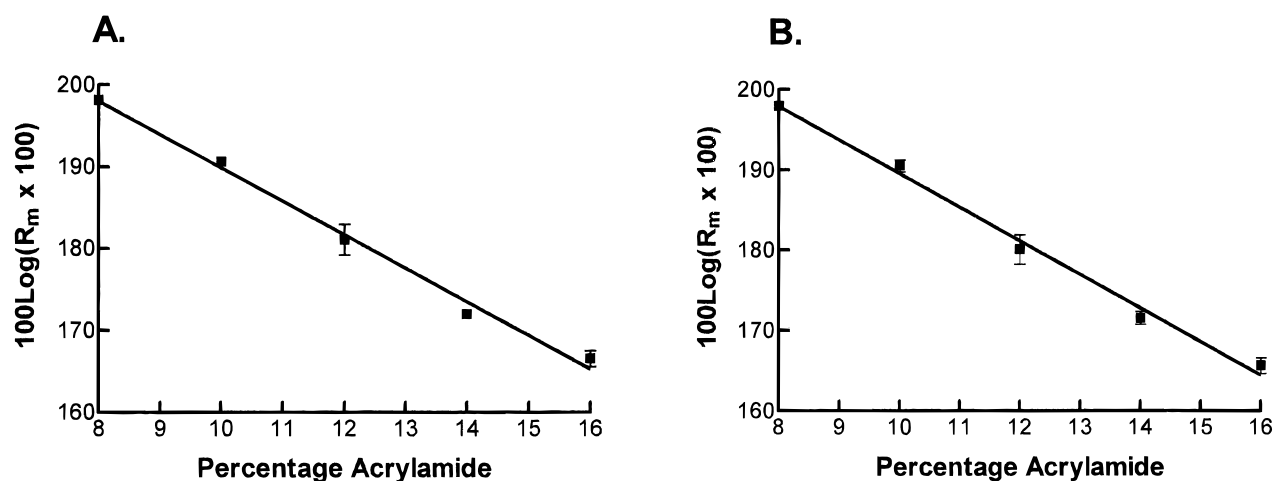

Fig. 3. Ferguson plots obtained with the wild-type and cys-less CTPs. The solubilized wild-type (panel A) and Cys-less (panel B) CTPs were electrophoresed at five different acrylamide concentrations ranging from 8 to 16%. Data were obtained from at least six independent observations at each point and are represented as means ± SD. Best-fit lines were constructed based on linear regression analysis via the methods of least squares. The resulting lines displayed the following parameters: Wild-type: slope = −4.09 ± 0.20; Y-axis intercept = 230.7 ± 2.5; correlation coefficient = 0.993; Cys-less: slope = −4.18 ± 0.20; Y-axis intercept = 231.3 ± 2.5; correlation coefficient = 0.993.

The data from both the size-exclusion chromatography and the charge-shift native gel electrophoresis are summarized in Table II. Our results clearly show that the solubilized wild-type and Cys-less CTPs display molecular weights which are quite close to the calculated value for the homodimer. We, therefore, conclude that upon solubilization the CTP exists as a homodimer. Moreover, these homodimers are functional upon incorporation into phospholipid vesicles. The most straightforward interpretation of these findings is that the homodimeric form of the CTP comprises a complete functional unit. This has important implications for the structural basis underlying the citrate translocation mechanism. For example, molecular modeling of the putative citrate translocation pathway(s) through the CTP must accommodate 12 rather than 6 membrane-spanning a-helical domains. Based on the above findings, we have recently initiated molecular modeling studies of the CTP. We generated helical wheel representations for all six TMDs and, for each helix, used hydropathy analysis to identify the most hydrophilic face. We modeled each TMD as a standard a-helix, with energy minimization to adjust for such factors as proline-induced bends. We have examined several possible ways in which a dimer might form. One such arrangement, which displays particularly favorable helix packing interactions, is illustrated in Fig. 4, in which the twelve TMDs form two seven-helix translocation channels. This model can be viewed interactively at the following web site: http://www.finchcms.edu/biochem/kaplan/ctp__model.html. The testing and refinement of such CTP models will be the focus of our future studies.
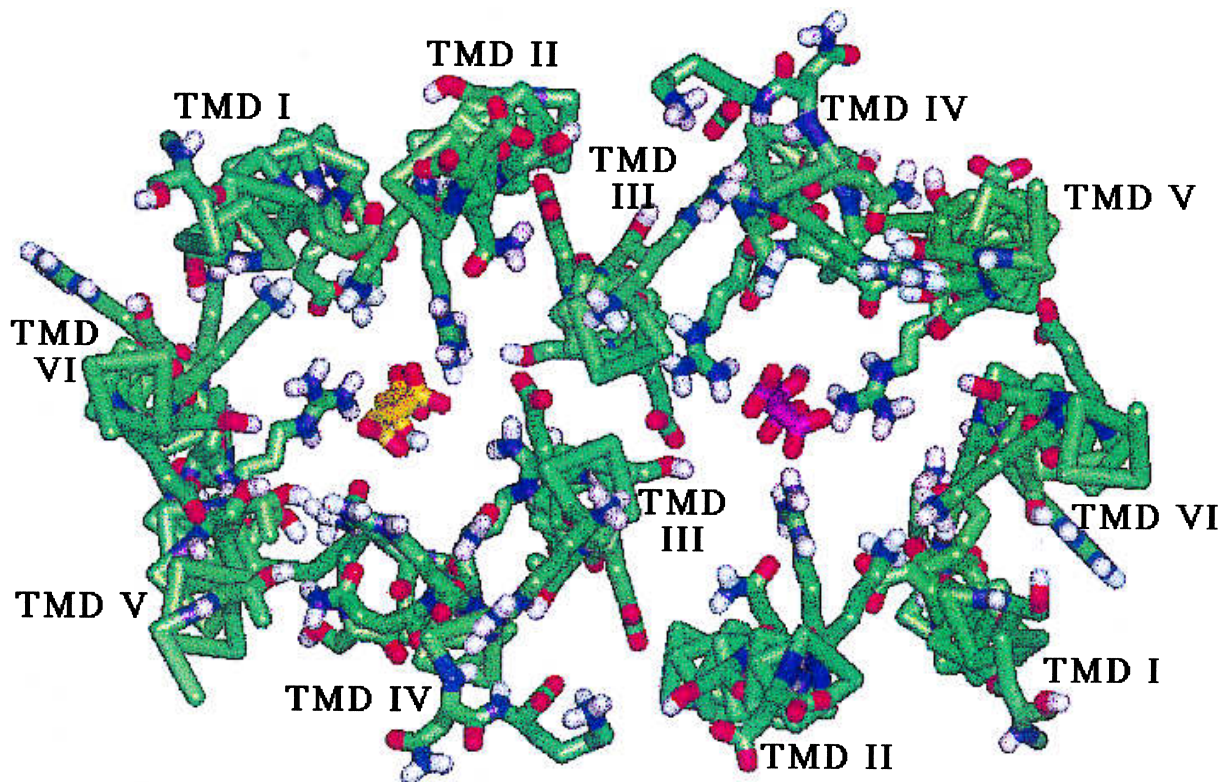
ACKNOWLEDGMENTS

Fig. 4. Stick figure model of the CTP dimer arranged clockwise to form two 7-helix pores. Only a-carbons, polar residues, and charged residues are shown, for clarity. View is from the top (outside) looking down through the CTP into the inner membrane as it projects towards the matrix (inside). Green denotes carbon atoms, white denotes hydrogen, blue denotes nitrogen, red denotes oxygen. A molecule of citrate (to scale; shaded in yellow) and isocitrate (cyan) are placed in each translocation pathway.

REFERENCES

Bisaccia, F., De Palma, A., and Palmieri, F. (1989). *Biochim. Biophys. Acta* **977**, 171–176.

Bisaccia, F., De Palma, A., Prezioso, G., and Palmieri, F. (1990). *Biochim. Biophys. Acta* **1019**, 250–256.

Bisaccia, F., Zara, V., Capobianco, L., Iacobazzi, V., Mazzeo, M., and Palmieri, F. (1996). *Biochim. Biophys. Acta* **1292**, 281–288.

Brunengraber, H., and Lowenstein, J. M. (1973). *FEBS Lett.* **36**, 130–132.

Bryan, J. K. (1977). *Anal. Biochem.* **78**, 513–519.

Chrambach, A., and Rodbard, D. (1971). *Science* **172**, 440–451.

Conover, T. E. (1987). *Trends Biochem. Sci.* **12**, 88–89.

Endemann, G., Goetz, P. G., Edmond, J., and Brunengraber, H. (1982). *J. Biol. Chem.* **257**, 3434–3440.

Ferguson, K. A. (1964). *Metabolism* **13**, 985–1002.

Hackenberg, H., and Klingenberg, M. (1980). *Biochemistry* **19**, 548–555.

Harlan, J. E., Picot, D., Loll, P. J., and Garavito, R. M. (1995). *Anal. Biochem.* **224**, 557–563.

Hedrick J. L., and Smith, A. J. (1968). *Arch. Biochem. Biophys.* **126**, 155–164.

Helenius, A., and Simons, K. (1977). *Proc. Natl. Acad. Sci USA* **74**, 529–532.

Kaplan, R. S. (1996). In *Molecular Biology of Membrane Transport Disorders* (Schultz, S. G., Andreoli, T. E., Brown, A. M., Fambrough, D. M., Hoffman, J. F., and Welsh, M. J., eds.), Plenum, New York, pp. 277–302.

Kaplan, R. S., and Pedersen, P. L. (1985). *Anal Biochem.* **150**, 97–104.

Kaplan, R. S., Pratt, R. D., and Pedersen, P. L. (1986). *J. Biol. Chem.* **261**, 12767–12773.

Kaplan, R. S., Mayor, J. A., Johnston, N., and Oliveira, D. L. (1990). *J. Biol. Chem.* **265**, 13379–13385.

Kaplan, R. S., Mayor, J. A., and Wood, D. O. (1993). *J. Biol. Chem.* **268**, 13682–13690

Kaplan, R. S., Mayor, J. A., Gremse D. A., and Wood, D. O. (1995). *J. Biol. Chem.* **270**, 4108–4114.

Klingenberg, M., and Appel, M. (1989). *Eur. J. Biochem.* **180**, 123–131.

Laemmli, U. K. (1970). *Nature London* **227**, 680–685.

Majima, E., Ikawa, K., Takeda, M., Hashimoto, M., Shinohara, Y., and Terada, H. (1995). *J. Biol. Chem.* **270**, 29548–29554.

Maloney, P. C. (1990). *Res. Microbiol.* **141**, 374–383.

Marger, M. D., and Saier, M. H. (1993). *Trends Biochem. Sci.* **18**, 13–20.

Newby, A. C., and Chrambach, A. (1979). *Biochem. J.* **177**, 623–630.

Palmieri, F., Stipani, I., Quagliariello, E., and Klingenberg, M. (1972). *Eur. J. Biochem.* **26**, 587–594.

Riccio, P., Aquila, H., and Klingenberg, M. (1975). *FEBS Lett.* **56**, 133–138.

Schagger, H., and von Jagow, G. (1991). *Anal. Biochem.* **199**, 223–231.

Schroers, A., Burkovski, A., Wohlrab, H., and Kramer, R. (1998). *J. Biol. Chem.* **273**, 14269–14276.

Watson, J. A., and Lowenstein, J. M. (1970). *J. Biol. Chem.* **245**, 5993–6002.

Xu, Y., Mayor, J. A., Gremse, D., Wood, D. O., and Kaplan, R. S. (1995). *Biochem. Biophys. Res. Commun* **207**, 783–789.

Xu, Y., Kakhniashvili, D. A., Gremse, D. A., Wood, D. O., Mayor, J. A., Walters, D. E., and Kaplan, R. S. (1999). *J. Biol. Chem.* Accepted for publication.